

## Cinnabaramides A–G: Analogues of Lactacystin and Salinosporamide from a Terrestrial Streptomyces

Marc Stadler,<sup>\*,†,‡</sup> Jens Bitzer,<sup>†</sup> Anke Mayer-Bartschmid,<sup>‡</sup> Hartwig Müller,<sup>‡</sup> Jordi Benet-Buchholz,<sup>§</sup> Florian Gantner,<sup>⊥</sup> Hans-Volker Tichy,<sup>||</sup> Peter Reinemer,<sup>∇</sup> and Kevin B. Bacon<sup>○</sup>

InterMed Discovery GmbH (IMD), Otto-Hahn-Strasse 15, D-44227 Dortmund, Germany, Bayer Health Care, Pharma Division, P.O.B. 101709, D-42096 Wuppertal, Germany, Institut Català d'Investigació Química, E-43007 Tarragona, Spain, Boehringer Ingelheim, Birkendorfer Strasse 65, 88397 D-Biberach, Germany, LUFA-ITL-GmbH, D-24116 Kiel, Germany, Proteros Biostructures GmbH, Am Klopferspitz 19, D-82152 Martinsried, Germany, and Actimis Pharmaceuticals, 11099 North Torrey Pines Road, Suite 200, La Jolla, California 92037

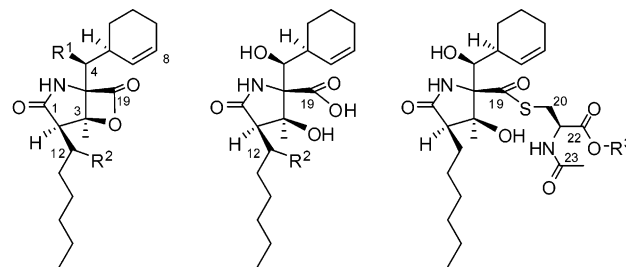
Received April 10, 2006

The cinnabaramides A–G (**1–7**) were isolated from a terrestrial strain of *Streptomyces* as potent and selective inhibitors of the human 20S proteasome. Their chemical and biological properties resemble those of salinosporamide A, a recently identified lead compound from an obligate marine actinomycete, which is currently under development as an anticancer agent. Cinnabaramides F and G (**6**, **7**) combine essential structural features of salinosporamide A and lactacystin and show about equal potency *in vitro*, with IC<sub>50</sub> values in the 1 nM range. The properties and phylogenetic position of the producer organism, the production and isolation of compounds **1–7**, their structure elucidation by MS and NMR, and their biological activities are reported. Additionally, an X-ray crystal structure was obtained from cinnabaramide A (**1**).

The proteasome is a highly conserved cellular structure, responsible for the nonlysosomal ATP-dependent proteolysis of most cellular proteins. The human 20S proteasome contains at least five distinct proteolytic activities, involving a threonine residue at the active site.<sup>1</sup> Although the 20S proteasome contains the proteolytic core, it cannot degrade proteins *in vivo* unless it is complexed with a 19S cap at either end of its structure, which itself contains multiple ATPase activities.<sup>1</sup> Due to their ability to inhibit NF- $\kappa$ B activation, proteasome inhibitors may be used to treat, for example, allergies, asthma, and cancers.<sup>2</sup> The proteasome inhibitor MS341/Velcade has received market approval for treatment of multiple myeloma.<sup>3</sup> Microorganisms that dwell in highly competitive environments have evolved various metabolites to address this ubiquitous target in eukaryotes.<sup>4,5</sup> Especially lactacystin from *Streptomyces lactacystineus*<sup>6</sup> and salinosporamide A from the obligate marine actinomycete *Salinispora tropica* (originally reported as "*Salinispora* sp.")<sup>7</sup> have raised considerable interest in the past years. Salinosporamide A in particular shows promising activities against multiple myeloma<sup>8</sup> and is currently under development as an anticancer drug.

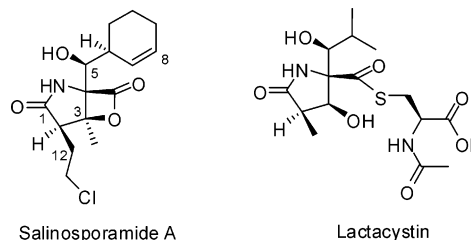
This work deals with the discovery of the cinnabaramides A–G (**1–7**), which are chemically related to both lactacystin and salinosporamide and were found during high-throughput screening of microbial extracts using a human 20S proteasome inhibitory assay.<sup>9</sup> An extract of strain JS360, isolated from soil collected in Japan, showed potent and selective activities. No concurrent inhibition of trypsin and chymotrypsin was observed. Neither the extract nor fractions derived thereof showed any significant activities in over 50 further protease and other biochemical high-throughput screening assays performed at Bayer HealthCare. This apparent selectivity of biological effects gave impetus to identify the active principles of strain JS360 and characterize the producer organism.

### Scheme 1



- 1** R<sup>1</sup> = OH, R<sup>2</sup> = H      **4** R<sup>2</sup> = OH  
**2** R<sup>1</sup> = R<sup>2</sup> = OH      **5** R<sup>2</sup> = H  
**3** R<sup>1</sup> = R<sup>2</sup> = H      **6** R<sup>3</sup> = H  
**7** R<sup>3</sup> = CH<sub>3</sub>

### Scheme 2



## Results and Discussion

To establish the molecular phylogeny of strain JS360, its 16S ribosomal DNA sequence was obtained.<sup>10</sup> A FASTA search revealed sequences of three terrestrial *Streptomyces* spp. (*S. cinnabarinus* and two isolates not identified at species level) each with 99% similarity to that of JS360 as closest matches. The aligned sequences were subjected to a similarity analysis (Figure 1), where they appeared rather distinct from those of *Salinispora*.<sup>11</sup> Strain JS360 showed highly similar morphological and biochemical properties to those of *S. cinnabarinus* DSM 40467. It is therefore a variant of that species or may be proven to constitute a new, closely related taxon in *Streptomyces*. These results are in agreement with the fact that the genus *Salinispora* is a member of the predominantly terrestrial actinomycete family Micromonosporaceae, which again is not too distantly related to *Streptomyces*.<sup>11</sup>

\* Corresponding author. Tel: +49(0)1520-8760217. Fax: +49(0)231-97426061. E-mail: marc.stadler@t-online.de.

<sup>†</sup> IMD.

<sup>‡</sup> Bayer HealthCare.

<sup>§</sup> Institut Català.

<sup>⊥</sup> Boehringer.

<sup>||</sup> Lufa.

<sup>∇</sup> Proteros.

<sup>○</sup> Actimis.

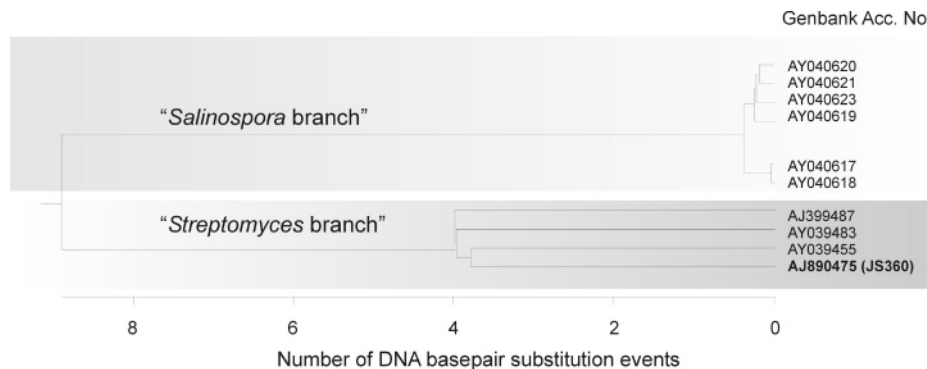


**Figure 1.** Phylogram revealing the phylogenetic distance between JS360, most similar sequences of other streptomycetes, and *Salinispora* spp. as inferred from a comparison of their 16S rDNA sequences (references obtained from GenBank<sup>9</sup>). The scale beneath the tree represents the distance between sequences.

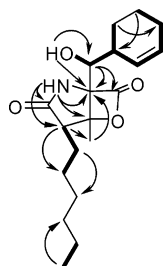


**Figure 2.** COSY (thick lines) and HMBC (arrows) correlations of cinnabaramide A (1).

Fermentation of strain JS360 was optimized in shake flasks and stirring fermentors to 30 L scale, allowing the production of cinnabaramide A in gram scale.<sup>9</sup> Only **1**–**6** were detected by HPLC-MS in the crude extracts, while **7** may have arisen from **6** during downstream processing. The compounds were obtained as described in the Experimental Section.

The most abundant component in the mycelium extract of strain JS360 was cinnabaramide A (**1**). HRESIMS provided the molecular formula  $C_{19}H_{29}NO_4$ , which was in accord with  $^{13}C$  NMR data. The  $^1H$  NMR spectrum showed the presence of a *cis* double bond ( $\delta_H$  5.73 and 5.81,  $^3J_{HH} = 10.4$  Hz), which was assigned to a cyclohexenyl ring by COSY and HMBC correlations (Figure 2). A methyl triplet ( $\delta_H$  0.87,  $^3J_{HH} = 6.7$  Hz) was found to constitute the end of a hexyl chain. Additional characteristic signals were derived from an amide proton ( $\delta_H$  8.91, s), an isolated methyl group ( $\delta_H$  1.74, s), and a methine proton ( $\delta_H$  2.41, dd). Detailed analysis of the corresponding 2D NMR data established the bicyclic core structure of compound **1**, including a  $\gamma$ -lactam ( $\delta_C$  175.9) and a  $\beta$ -lactone ( $\delta_C$  168.9) moiety. The position of the hexyl substituent at C-2 was indicated by a cross-peak in the COSY spectrum and by long-range CH coupling between 2-H and C-13. Finally, a methine group ( $\delta_H$  3.67) bearing a hydroxy moiety ( $\delta_H$  5.49) was identified as a linkage between the cyclohexenyl ring and C-4 and established the planar structure of cinnabaramide A (**1**). The structure resembles that of salinosporamide A,<sup>7</sup> except for the chloroethyl moiety, which is replaced by a hexyl residue.

The absolute and relative configuration of **1** was obtained from an X-ray diffraction analysis.<sup>12</sup> A suitable crystal was obtained by slow evaporation of a saturated solution of **1** in propanol/diacetone alcohol (97:3) at 46 °C. Cinnabaramide A (**1**) crystallized in the chiral orthorhombic space group  $P2_12_12_1$ . The crystal cell had exceptionally large dimensions and contained 12 independent molecules with identical chirality, all of which showed conformational differences (Figure 3a). The molecules were packed in polar and nonpolar layers (Figure 3b), with the polar layers being connected two-dimensionally through a framework of hydrogen bonds. The absolute configuration of **1** was determined as 2*R*, 3*S*, 4*R*, 5*S*, 6*S* using Cu  $K\alpha$  radiation [Flack parameter: 0.02 (0.19)].

Thus, the absolute configuration of **1** agrees with that of salinosporamide A.<sup>7</sup>

The  $^1H$  NMR spectrum of cinnabaramide B (**2**) was similar to that of **1** and displayed most of the diagnostic resonances present there. A difference was found in the coupling pattern of H-2 ( $\delta_H$  2.35, d instead of dd), which was explained by an additional hydroxy group at C-12 ( $\delta_H$  4.67) of the hexyl chain. HRESIMS revealed the molecular formula  $C_{19}H_{29}NO_5$ , thus providing additional evidence for cinnabaramide B (**2**) being the 12-OH derivative of **1**. Because of the free rotation of the hexyl chain, the configuration at C-12 could not be established by NMR. Preparation and analysis of a Mosher's ester seemed promising to define this configuration, as the competing 5-OH should be sterically hindered.<sup>7</sup> However, initial attempts at preparing a Mosher's ester, using either dichloromethane/Huenig's base or pyridine, did not lead to conversion or failed to discriminate between the two hydroxy groups, respectively. Contrary to **2**, cinnabaramide C (**3**) had one hydroxy group less than **1**, as suggested by its molecular weight of 331 g/mol and the HRMS-derived formula  $C_{19}H_{29}NO_3$ . Analysis of the NMR spectra revealed the presence of a methylene group ( $\delta_H$  1.76) between bicyclic and cyclohexenyl moieties, thus proving **3** to be the 5-deoxy derivative of **1**. On the basis of similar specific rotations for **2** and **3** compared with **1**, and of  $^1H$  coupling constant analysis, the stereocenters of these compounds are assumed to have identical relative and absolute configurations.

Cinnabaramides D (**4**) and E (**5**) showed similar NMR spectra to **2** and **1**, respectively. HRMS data revealed that **4** and **5** each possess two additional hydrogen atoms, suggesting that these molecules constitute *seco*-forms of the corresponding  $\beta$ -lactone moieties. This presumption was proven by the presence of an additional hydroxy proton ( $\delta_H$  5.39 and 4.79, respectively) showing the expected HMBC couplings and a free carboxyl group ( $\delta_H$  12.52 and 12.44, respectively). Interestingly, the specific rotation of **5** was significantly smaller than the values obtained for **1**–**3**, and **4** did not show any optical activity. This points to a facilitated epimerization of these metabolites, although it remains unclear which stereocenters are affected.

The NMR spectra of **6** and **7** showed a complete new subset of resonances that proved to belong to an *N*-acylated cysteine residue, which is linked to the core structure via a thioester bond with the carbonyl group of the former  $\beta$ -lactone. The thioester moiety was identified by the downfield chemical shift ( $\delta_C > 200$ ) of a *cis*-carbonyl carbon, and by the HMBC derived connectivity to the  $\beta$ -hydrogens of cysteine. The chirality of this residue was determined by Marfeys method as L-cysteine. Compound **7** exhibited an additional methoxy resonance ( $\delta_H$  3.59), which showed an HMBC cross-peak with the cysteine carbonyl group ( $\delta_C$  171.0). Thus, cinnabaramide G (**7**) is the methyl ester of cinnabaramide F (**6**). Compound **7** could not be detected by HPLC in the crude extracts and is therefore considered to be an artifact of the isolation

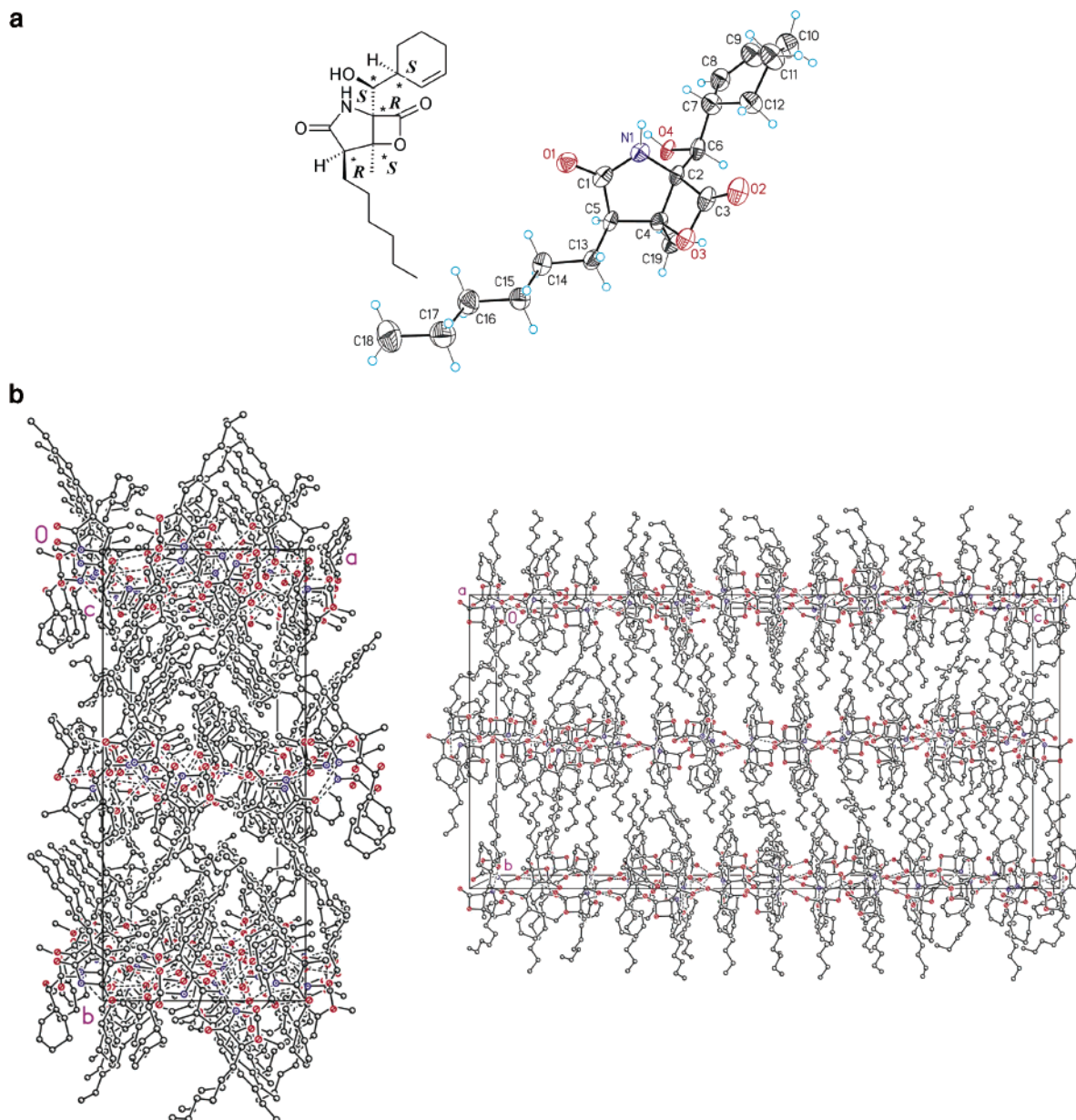


**Figure 3.** (a) ORTEP plot (50%) of cinnabaramide A (**1**) and structure showing the absolute configuration. (b) Crystal packing of cinnabaramide A (**1**) with view along the *a* (right) and *c* (left) axes, showing the polar and nonpolar layers.

procedure. Because both **6** and **7** can easily be obtained from **1** by nucleophilic attack of the thiol group at the  $\beta$ -lactone,<sup>9</sup> it seems likely that the stereocenters of the core structure retain their configurations. However, their specific rotation values show opposite signs compared with **1**, probably due to the additional chiral residue. Both **6** and **7** are analogues of lactacystin, a metabolite also produced by a terrestrial *Streptomyces* species. Like the other cinnabaramides (**1–5**), **6** and **7** also feature essential structural characteristics of the salinosporamides and thus can be regarded as “chimeric” structures.

The cinnabaramides A–G (**1–7**) strongly inhibited the proteasome (Table 1), but did not show any activity against trypsin and chymotrypsin up to 100  $\mu$ M. The  $IC_{50}$  of **1** was 1 nM, suggesting a similar potency to that reported for salinosporamide A.<sup>7</sup> The other  $\beta$ -lactones (**2**, **3**) still had inhibitory effects in the low nM range, while the corresponding *seco*-forms (**4**, **5**) showed substantially decreased bioactivities. Interestingly, **6** and **7** were as potent as **1**, suggesting a “prodrug-like” mechanism as postulated for the analogous lactacystin,<sup>13</sup> which, however, showed weaker target activities than all cinnabaramides (Table 1). This observation complements our knowledge of the structure–activity relationships

**Table 1.** Activities of Cinnabaramides A–G (**1–7**) and Lactacystin in a Human 20S Proteasome Inhibitory Assay<sup>9</sup>

compound	$IC_{50}$ [nM]
<b>1</b>	1
<b>2</b>	245
<b>3</b>	12
<b>4</b>	100
<b>5</b>	136
<b>6</b>	6
<b>7</b>	0.6
lactacystin	259

of the cinnabaramide/salinosporamide metabolite family<sup>14</sup> and offers interesting options for synthetic and semisynthetic optimizations: Preliminary stability studies (incubation in horse serum or water supplied with 20% MeOH solutions of compounds **1–3** and **6/7** at pH 4, 7, and 10, respectively) revealed their long-term stability under acidic conditions. Those cinnabaramides possessing a  $\beta$ -lactone moiety (**1–3**) immediately decayed in the alkaline range, while being only moderately stable (50–65% recovery after 24 h incubation as estimated by HPLC) in the neutral pH range. Under



such conditions, the cinnabaramides **6** and **7** were more stable than the lactones (over 90% recovery at neutral pH and ca. 45% at alkaline pH after 48 h). HPLC analyses of **1–3** further suggested that the lactones had opened to the corresponding *seco*-forms, whose biological effects are substantially reduced (see Table 1). Masking the  $\beta$ -lactones by further thiols (or other substituents with comparable nucleophilic properties) may thus enhance the potency of resulting derivatives by increasing their stability.

Groll et al. have recently evaluated the X-ray crystal structures of salinosporamides A and B in a complex with the 20S proteasome.<sup>15</sup> Their studies revealed important information for the lactone ring opening, and it was postulated that the chlorine in salinosporamide A serves as a leaving group, rendering the binding of the salinosporamide molecule to the proteasome irreversible. From a comparison of *in vitro* data, which revealed about equal potency of the most potent cinnabaramides (**1** and **7**) and salinosporamide A (activities in the 1 nM range in both cases, using essentially the same assay conditions; see Table 1 and ref 7), the chlorine found in salinosporamide A does not appear to be essential for potent *in vitro* proteasome inhibition. The cinnabaramides A–G (**1–7**) have not yet been subjected to mechanistic studies similar to those performed in ref 15. On the other hand, salinosporamide A was not available for comparison to us; hence it is difficult to interpret as to whether the strength of target binding is actually correlated to the results seen in the target-based biological assay. These discrepancies of our *in vitro* data to the results reported in ref 15 therefore remain to be validated by concurrent testing of both classes of compounds, including a comparison of their stability in biological systems and evaluation of further pharmacokinetic data. Nevertheless, this work revealed that terrestrial actinomycetes may yield similar lead compounds to those that have recently been obtained from their marine counterparts.

Notably, the effects of **1–7** in some cellular assays were substantially weaker than expected. For example, the IC<sub>50</sub> of **1** was only 500 nM for LPS-induced inhibition of TNF  $\alpha$  production in human PMBC cells, and its cytotoxicity against MDA-MB 231 and H460 cells<sup>9</sup> was determined in the range of IC<sub>50</sub> = 1  $\mu$ M. The activities of **1** against the HCT-116 cell line, however, were found to be as potent as described for salinosporamide A,<sup>7</sup> i.e., in the 10 nM range, suggesting that this type of colon cancer is particularly susceptible to this class of compounds.

The discrepancies of target and cellular activities suggest that the cinnabaramides have limited cell permeability and/or stability under the assay conditions employed. This needs to be confirmed by additional data, but apparent selectivity against particular cancers could even constitute an advantage. Chemotherapeutic agents that leave normally proliferating cells unaffected appear more promising than compounds showing a broad, general cytotoxicity. Extensive studies on their selectivity toward malignant cell lines, along with improvements of their activity and selectivity by means of medicinal chemistry, may eventually result in potent anticancer drugs based on the salinosporamide/cinnabaramide family. Various promising synthetic approaches have recently been realized.<sup>16</sup> Additionally, strong antifungal and insecticidal activities for this compound class are claimed in a patent application, which could serve as a starting point for the development of a new class of agrochemicals.<sup>17</sup> Details on this subject will be reported separately.

## Experimental Section

**General Experimental Procedures.** Chemicals were obtained in analytical grade from Merck (Darmstadt, Germany) or Sigma-Aldrich (Deisenhofen, Germany), if not indicated otherwise. Optical rotations were measured in MeOH with a Perkin-Elmer 341 polarimeter, and UV spectra with a Biochrom Ultraspec 2000 spectrometer. IR spectra were obtained on a Perkin-Elmer Spectrum BX FTIR spectrometer equipped with an attenuated total reflection (ATR) accessory (DuraSampIR II, SensIR Technologies). NMR spectra were recorded in DMSO-*d*<sub>6</sub> on a Bruker DRX500 spectrometer at 300 K, operating at

500.13 MHz proton frequency. The solvent peak was used as internal reference ( $\delta_{\text{H}}$  2.50,  $\delta_{\text{C}}$  39.5). Analytical and preparative HPLC were performed using the previously described equipment and methodology.<sup>9,23</sup> Briefly, for HPLC-UV/vis an HP 1100 (Agilent) equipped with a Merck LiChroSpher C18 column (5  $\mu$ m, 125  $\times$  4 mm) and a linear gradient from 0 to 100% acetonitrile (MeCN) (0.01% H<sub>3</sub>PO<sub>4</sub>, flow rate 1 mL/min) in 10 min was used; HPLC-MS and HPLC-HRMS were performed on an HP1100 coupled with a LCT mass spectrometer (Micromass, Manchester, UK) in positive and negative ESI mode, using a Waters Symmetry C18 column (3.5  $\mu$ m, 50  $\times$  2.1 mm) and a linear gradient from 0 to 100% MeCN (0.1% HCOOH, flow rate 0.5 mL/min) in 12 min. For amino acid analysis, the same equipment was used with a Waters Symmetry C18 column (3.5  $\mu$ m, 150  $\times$  2.1 mm) and a linear gradient from 5 to 40% MeCN (0.1% HCOOH, flow rate 0.5 mL/min) in 40 min. Preparative HPLC methods are specified below in detail.

**Characterization and Maintenance of Strain JS360.** The actinomycete strain JS360 was obtained in 1991 from a soil sample collected in Japan, using a conventional isolation procedure. It has been deposited at DSMZ (Braunschweig, Germany) as DSM 15324. For evaluation of its molecular taxonomy, the major part of the 16S rRNA gene was amplified. Amplification products were purified using DNA-binding paramagnetic beads (Mag Prep PCR clean up kit, Tecan, Hornbrechtikon, Switzerland), following the manufacturer's recommendation. Nucleotide sequences were obtained by cycle sequencing using the Thermo Sequenase Cy5.5 dye terminator cycle sequencing kit (Amersham), primer 41f, and the LI-COR 4200 genetic analyzer (LI-COR, Lincoln, NE). A 240 bp DNA sequence was obtained and used as a FASTA input to search for similar sequences in GenBank.<sup>10</sup> The closest matches (99% similarity) were found for *S. cinnabarinus* (sequence AJ399487) and two unidentified *Streptomyces* spp. (AY039455, AY039483) from soil and an earthworm, respectively. These sequences as well as sequences of *Salinispora* spp. (designations in GenBank: AY040617, AY040618, AY040619, AY040620, AY040621, AY040623) were used as input for the MegAlign module of the LASERGENE software (DNASTAR Inc., Madison, WI).

**Production and Isolation of Cinnabaramides.** Strain JS360 was propagated using YMG (D-glucose 0.4%, malt extract 1%, yeast extract 0.4%, pH 7.2) and Q6 media (D-glucose 0.5%, glycerol 2%, cottonseed meal 1%, CaCO<sub>3</sub> 0.1%, pH 7.2). Further culture media in which production of **1–7** occurred are described in the patent literature.<sup>9</sup> Q6 was chosen for scale-up because it led to the highest production rates, as monitored by quantitative HPLC. Aside from compounds **1–7**, no other metabolites chemically related to this group were observed by analytical HPLC, and the bioassay-guided fractionation also suggested that **1–7** are the only active principles produced by JS360 under the described fermentation conditions.

As seed cultures for scale-up fermentations, 2.0 mL of a mycelial suspension of strain JS360 in 10% glycerol was used to inoculate 1 L Erlenmeyer flasks containing 150 mL of sterile YMG medium and propagated on a rotary shaker at 28 °C and 240 rpm for 76 h. A 40 L Biostat P fermentor (Braun Bioengineering, Melsungen, Germany) containing 30 L of Q6 medium was sterilized (1 h, 121 °C, 1 bar) and inoculated with two well-grown YMG seed cultures. The production culture was grown under stirring (240 rpm) and aeration (0.3 vvm) at 28 °C. Cinnabaramides were already detected by HPLC analyses of crude EtOAc extracts of the culture broth after 70 h of fermentation, but production reached a maximum at 120 h. After harvesting, mycelium and culture fluid were separated by centrifugation (10 min at 1000g). The culture filtrate was applied onto a column filled with 1 kg of Lewapol CA 9225 adsorption resin (Bayer, Leverkusen, Germany), which was washed with 5 L of H<sub>2</sub>O. The column was eluted with 6 L of acetone/MeOH, 4:1. The eluate was concentrated *in vacuo* (40 °C) to yield an aqueous residue, which was diluted to 1 L with H<sub>2</sub>O and extracted with 3  $\times$  1 L of EtOAc. The combined organic phases were dried over Na<sub>2</sub>SO<sub>4</sub>. The solvent was removed *in vacuo* (40 °C), resulting in 22.7 g of crude extract. The mycelium was extracted for 1 h with acetone (3  $\times$  5 L). The solvent was removed *in vacuo* (40 °C), and the aqueous residue was treated as the culture filtrate extract to yield 13.4 g of dry residue.

Aliquots of 2.5–3 g of these oily crude extracts were dissolved in 5 mL of MeOH and filtered through a Bond Elut C18 500 mg cartridge (Baker, Deventer, Netherlands) to remove lipophilic constituents, and the eluates were applied onto a MZ Analysetechnik (Mainz, Germany)

**Table 2.** NMR Data (500 MHz, DMSO-*d*<sub>6</sub>) for Cinnabaramides A–E (1–5)

position	cinnabaramide A (1)		cinnabaramide B (2)		cinnabaramide C (3)		cinnabaramide D (4)		cinnabaramide E (5)	
	$\delta_C$ , mult.	$\delta_H$ (J in Hz)	$\delta_C$ , mult.	$\delta_H$ (J in Hz)	$\delta_C$ , mult.	$\delta_H$ (J in Hz)	$\delta_C$ , mult.	$\delta_H$ (J in Hz)	$\delta_C$ , mult.	$\delta_H$ (J in Hz)
1	175.9, qC		171.9, qC		175.6, qC		176.8, qC		177.7, qC	
2	47.7, CH	2.41, dd (7.6, 5.8)	54.7, CH	2.35, d (2.6)	46.9, CH	2.56, dd (7.7, 5.8)	53.3, CH	2.47, d (5.4)	50.5, CH	2.45, t (6.1)
3	86.1, qC		75.9, qC		86.1, qC		80.6, qC		80.3, qC	
4	78.6, qC		69.2, qC		74.3, qC		76.0, qC		75.5, qC	
5	69.1, CH	3.67, dd (9.0, 7.8)	75.1, CH	3.53, d (9.5)	32.5, CH <sub>2</sub>	1.79, m	74.6, CH	3.72, t (7.0)	74.7, CH	3.75, d (6.1)
6	37.7, CH	2.29, m	36.3, CH	2.79, m	29.8, CH	2.27, m	38.5, CH	2.12, m	38.6, CH	2.12, m
7	128.5, CH	5.81, m	128.0, CH	5.90, m	131.1, CH	5.44, m	129.3, CH	5.80, m	129.3, CH	5.82, m
8	127.7, CH	5.73, m	127.9, CH	5.69, m	127.6, CH	5.68, m	127.1, CH	5.64, m	127.2, CH	5.65, m
9	24.6, CH <sub>2</sub>	1.92, m	24.4, CH <sub>2</sub>	1.92, m	24.4, CH <sub>2</sub>	1.92, m	24.3, CH <sub>2</sub>	1.88, m	24.5, CH <sub>2</sub>	1.88, m
10	21.0, CH <sub>2</sub>	1.41, 1.70, m	21.4, CH <sub>2</sub>	1.49, 1.77, m	20.2, CH <sub>2</sub>	1.47, 1.65, m	21.5, CH <sub>2</sub>	1.36, 1.66, m	21.6, CH <sub>2</sub>	1.36, 1.67, m
11	25.3, CH <sub>2</sub>	1.24, 1.82, m	28.9, CH <sub>2</sub>	1.60, 1.71, m	28.7, CH <sub>2</sub>	1.25, 1.87, m	26.2, CH <sub>2</sub>	1.21, 1.68, m	26.4, CH <sub>2</sub>	1.25, 1.66, m
12	24.7, CH <sub>2</sub>	1.49, 1.60, m	76.6, CH	4.67, m	24.7, CH <sub>2</sub>	1.51, 1.62, m	68.0, CH	3.85, m	23.4, CH <sub>2</sub>	1.34, 1.51, m
13	27.0, CH <sub>2</sub>	1.45, 1.53, m	32.0, CH <sub>2</sub>	1.56, 1.59, m	27.0, CH <sub>2</sub>	1.45, 1.52, m	34.4, CH <sub>2</sub>	1.66, m	28.2, CH <sub>2</sub>	1.32, 1.44, m
14	28.8, CH <sub>2</sub>	1.29, m	24.1, CH <sub>2</sub>	1.37, m	28.7, CH <sub>2</sub>	1.30, m	24.5, CH <sub>2</sub>	1.25, 1.38, m	29.1, CH <sub>2</sub>	1.25, m
15	31.0, CH <sub>2</sub>	1.28, m	30.8, CH <sub>2</sub>	1.28, m	31.0, CH <sub>2</sub>	1.28, m	31.3, CH <sub>2</sub>	1.25, m	31.2, CH <sub>2</sub>	1.25, m
16	22.0, CH <sub>2</sub>	1.28, m	21.9, CH <sub>2</sub>	1.29, m	22.0, CH <sub>2</sub>	1.28, m	22.1, CH <sub>2</sub>	1.28, m	22.1, CH <sub>2</sub>	1.26, m
17	13.9, CH <sub>3</sub>	0.87, t (6.7)	13.8, CH <sub>3</sub>	0.87, t (6.7)	13.9, CH <sub>3</sub>	0.87, t (6.7)	14.0, CH <sub>3</sub>	0.87, t (7.0)	14.0, CH <sub>3</sub>	0.87, t (6.8)
18	20.0, CH <sub>3</sub>	1.74, s	21.0, CH <sub>3</sub>	1.35, s	19.2, CH <sub>3</sub>	1.61, s	21.0, CH <sub>3</sub>	1.51, s	20.5, CH <sub>3</sub>	1.46, s
19	168.9, qC		170.8, qC		170.1, qC		171.6, qC	12.52, <sup>a</sup> br, s	172.2, qC	12.44, <sup>a</sup> br, s
NH		8.91, s		8.52, s		8.99, s		8.12, s		7.65, s
3-OH								5.39, s		4.80, br, s
5-OH		5.49, d (7.9)		6.11, s				4.91, d (7.6)		4.80, m
12-OH				4.00, br, s				5.28, br, s		

<sup>a</sup> COOH

**Table 3.** NMR Data (500 MHz, DMSO-*d*<sub>6</sub>) for Cinnabaramides F and G (6, 7)

position	cinnabaramide F (6)		cinnabaramide G (7)	
	$\delta_C$ , mult.	$\delta_H$ (J in Hz)	$\delta_C$ , mult.	$\delta_H$ (J in Hz)
1	179.0, qC		179.1, qC	
2	50.6, CH	2.47, t (6.2)	50.6, CH	2.45, t (6.4)
3	80.8, qC		80.8, qC	
4	80.1, qC		80.1, qC	
5	75.5, CH	3.78, d (6.4)	75.5, CH	3.78, t (7.0)
6	38.2, CH	2.12, m	38.1, CH	2.13, m
7	129.3, CH	5.79, m	129.2, CH	5.79, m
8	127.3, CH	5.63, m	127.2, CH	5.63, m
9	24.5, CH <sub>2</sub>	1.85, m	24.5, CH <sub>2</sub>	1.85, m
10	21.4, CH <sub>2</sub>	1.33, 1.62, m	21.4, CH <sub>2</sub>	1.33, 1.61, m
11	27.1, CH <sub>2</sub>	1.08, 1.64, m	27.1, CH <sub>2</sub>	1.08, 1.62, m
12	23.4, CH <sub>2</sub>	1.36, 1.46, m	23.4, CH <sub>2</sub>	1.35, 1.45, m
13	28.1, CH <sub>2</sub>	1.35, 1.50, m	28.1, CH <sub>2</sub>	1.34, 1.49, m
14	29.0, CH <sub>2</sub>	1.24, m	29.0, CH <sub>2</sub>	1.24, m
15	31.2, CH <sub>2</sub>	1.25, m	31.2, CH <sub>2</sub>	1.25, m
16	22.1, CH <sub>2</sub>	1.27, m	22.1, CH <sub>2</sub>	1.26, m
17	14.0, CH <sub>3</sub>	0.86, t (6.7)	14.1, CH <sub>3</sub>	0.86, t (6.7)
18	20.9, CH <sub>3</sub>	1.43, s	20.9, CH <sub>3</sub>	1.43, s
19	201.1, qC <sup>a</sup>		201.3, qC <sup>a,b</sup>	
20	29.7, CH <sub>2</sub>	2.97, dd (13.4, 7.8), 3.28, m	29.4, CH <sub>2</sub>	2.99, dd (13.4, 8.2), 3.24, m
21	51.4, CH	4.36, m	51.5, CH	4.39, m
22	171.9, qC	12.77, br, s <sup>c</sup>	171.0, qC	
23	169.3, qC		169.3, qC	
24	22.4, CH <sub>3</sub>	1.82, s	22.3, CH <sub>3</sub>	1.83, s
OMe			52.1, CH <sub>3</sub>	3.64, s
NH		8.21, s		8.21, s
Cys-NH		8.01, d (8.2)		8.21, d (7.6)
3-OH		4.75, br, s		4.76, br, s
5-OH		5.01, br, s		5.02, d (7.1)

<sup>a</sup> Broad resonance. <sup>b</sup> <sup>13</sup>C chemical shift obtained from HMBC experiment. <sup>c</sup> COOH.

Kromasil RP 18 column (7  $\mu$ m, 250  $\times$  40 mm). A linear gradient of 20–50% MeCN (0.01% TFA) in 40 min was applied at a flow of 10 mL/min; thereafter a linear gradient from 50 to 100% MeCN in 20 min; thereafter isocratic conditions at 100% MeCN for 30 min. Five intermediate products (IP A–E) were eluted subsequently and obtained by fractionation according to UV adsorption at 210 nm: IP A at  $t_R$  = 61–64 min (containing 4 and 7), IP B at  $t_R$  = 65–71 min (containing 5 and 6), IP C at  $t_R$  = 72–79 min (containing 2), IP D at  $t_R$  = 79–85 min (containing 1), and IP E at  $t_R$  = 86–93 min (containing 3). Final purification of active components in these intermediate products was achieved by a second preparative HPLC step, using the same mobile phase at a flow of 7 mL/min, a MZ Analysentechnik Inertsil C18 column (7  $\mu$ m, 250  $\times$  30 mm), and the following gradient: isocratic conditions (30% MeCN) for 30 min; thereafter linear gradient from 30 to 100% MeCN in 50 min, thereafter isocratic conditions (100% MeCN) for 20 min. Yields and  $t_R$ 's of cinnabaramides A–G (1–7) are summarized in Table S1 (Supporting Information).

**X-ray Crystal Data for Cinnabaramide A (1).** Data collection: Bruker-Nonius diffractometer equipped with a Proteum CCD area detector, a FR591 rotating anode with Cu K $\alpha$  radiation, Montel mirrors as monochromator, and a Kryoflex low-temperature device ( $T$  = 90 K). Full-sphere data collection  $\omega$  and  $\varphi$  scans were used. Crystal data: C<sub>19</sub>H<sub>29</sub>N<sub>1</sub>O<sub>4</sub>  $\times$  12,  $M_r$  = 335.26 (4023.17); orthorhombic; space group  $P2_12_12_1$ ,  $a$  = 13.0624(2)  $\text{\AA}$ ,  $b$  = 29.0543(5)  $\text{\AA}$ ,  $c$  = 58.4559(11)  $\text{\AA}$ ,  $V$  = 22178.2(7)  $\text{\AA}^3$ ,  $Z$  = 4,  $\rho_{\text{calc}}$  = 1.205 Mg/m<sup>3</sup>,  $\mu$  = 0.674 mm<sup>-1</sup>. Reflections measured 205 845, 26 995 unique reflections ( $R_{\text{int}}$  = 0.1073), 21 119  $F_o > 4\sigma(F_o)$ , goodness-of-fit on  $F^2$  = 1.076,  $R_1$  = 0.0781 (0.1039),  $wR_2$  = 0.1832 (0.1989), 2674 refined parameters, largest diff peak (hole) = 0.431 (–0.385) e  $\text{\AA}^{-3}$ , measurement range 4.69–54.33° (Cu K $\alpha$  radiation), Flack: 0.0(2). Programs used: Data collection Proteum V. 1.37 (Bruker-Nonius 2002), data reduction Saint Plus Version 1.6 (Bruker-Nonius 2002), and absorption correction SADABS V. 2.03 (2002). Structure solution and refinement was accomplished using SHELXTL software Version 6.10.<sup>18</sup>

**Amino Acid Analysis.** The absolute configuration of the cysteine residue was determined according to Marfey's method.<sup>19</sup> Compound 6 (0.5 mg) was hydrolyzed in 6 N HCl (500  $\mu$ L) for 20 h at RT. After drying under argon flow the residue was resolved in 200  $\mu$ L of acetone/H<sub>2</sub>O (1:1). FDAA solution (100  $\mu$ L, 1% in acetone) and Na<sub>2</sub>CO<sub>3</sub> (20  $\mu$ L, 1M) were added, and the mixture was incubated for 1 h at 40  $^{\circ}$ C.

After cooling to RT, 10  $\mu$ L of 2 N HCl was added and the solution directly applied to HPLC-MS as described above.

**Biological Assays.** For the proteasome inhibition assay, the compounds were diluted at various concentrations in 2.5% DMSO in polypropylene 96-well plates, with MG-132 (Peptide Institute, Osaka, Japan) as internal control. The diluted working solution (10  $\mu$ L/well) was transferred into a polypropylene 96-well plate. The assay buffer was composed of 50 mM Tris-HCl (pH 8.0), 0.5 mM EDTA, 0.005% TritonX-100, and 0.005% SDS, prepared as a stock solution at 10 $\times$  concentration. The peptide substrate (Suc-Leu-Leu-Val-Tyr-MCA; 3120v; Peptide Institute, Osaka, Japan) was stored at 10 mM in 100% DMSO and diluted at 125  $\mu$ M in 1.25 $\times$  concentration of the assay buffer. For testing, 40  $\mu$ L of the substrate solution was added to the compound solution. The compound and the substrate were preincubated for 10 min at RT. Then the mixture of the compound and the substrate (10  $\mu$ L/well) was transferred to a black noncoated 384-well assay plate (Nunc) and autofluorescence emission measured at 460 nm ( $\lambda_{\text{exc}}$ , 360 nm), using a ARVO fluorescence plate reader (Perkin-Elmer). Human red blood cell S20 proteasome (Affinity Research Products, Exeter, UK) was diluted 1 in 1000 with 1 $\times$  concentration of the assay buffer and 10  $\mu$ L added to the substrate/inhibitor mixture in the plate. The proteolytic reaction was performed at RT. The fluorescence emission was continuously measured for 90 min. IC<sub>50</sub> values were determined at initial velocity of the reaction.

For determination of lipopolysaccharide (LPS)-induced TNF $\alpha$  release, peripheral mononuclear cells (PBMC) were isolated from heparinized blood of healthy donors by standard density-gradient centrifugation on 80% Percoll (Amersham, Uppsala, Sweden) diluted in phosphate-buffered saline (PBS). PBMC were washed twice in PBS, resuspended in RPMI1640 medium supplemented with 10% heat-inactivated fetal calf serum (JRH, Biosciences, Lenexa, KS), 292 mg/mL L-glutamine (Invitrogen, Carlsbad, CA), 100 IU/mL penicillin G, and 100 mg/mL streptomycin, and preincubated for 1 h with test compound or the corresponding volume of solvent (DMSO, final concentrations 0.1%) before the addition of LPS (1  $\mu$ g/mL). After overnight culture, supernatants were collected and TNF- $\alpha$  concentrations determined by ELISA, following the manufacturer's recommendations (Genzyme Techné, Cambridge, MA).

**Cinnabaramide A (1):** white crystals;  $[\alpha]_D^{20}$  –93 (c 0.5, MeOH); UV (MeOH)  $\lambda_{\text{max}}$  (log  $\epsilon$ ) 202 (4.24), 227 (3.68) nm; IR (ATR)  $\nu_{\text{max}}$



2929, 1812, 1702, 1382, 1349, 1308, 1225, 1020, 829  $\text{cm}^{-1}$ ; NMR data, see Table 2; HRESIMS  $m/z$  336.2178 (calcd for  $\text{C}_{19}\text{H}_{30}\text{NO}_4$   $[\text{M} + \text{H}]^+$ , 336.2171,  $\Delta$  2.1 ppm).

**Cinnabaramide B (2):** white, amorphous solid;  $[\alpha]_D^{20}$   $-140$  ( $c$  0.5, MeOH); UV (MeOH)  $\lambda_{\text{max}}$  (log  $\epsilon$ ) 201 (4.12), 225 (3.54) nm; IR (ATR)  $\nu_{\text{max}}$  2929, 1702, 1380, 1314, 1192, 1133, 1050, 1023, 823  $\text{cm}^{-1}$ ; NMR data, see Table 2; HRESIMS  $m/z$  352.2136 (calcd for  $\text{C}_{19}\text{H}_{30}\text{NO}_5$   $[\text{M} + \text{H}]^+$ , 352.2119,  $\Delta$  4.8 ppm).

**Cinnabaramide C (3):** white, amorphous solid;  $[\alpha]_D^{20}$   $-80$  ( $c$  0.5, MeOH); UV (MeOH)  $\lambda_{\text{max}}$  (log  $\epsilon$ ) 202 (4.19), 223 (3.76) nm; IR (ATR)  $\nu_{\text{max}}$  2927, 1816, 1698, 1345, 1146, 1113, 1036, 825  $\text{cm}^{-1}$ ; NMR data, see Table 2; HRESIMS  $m/z$  320.2220 (calcd for  $\text{C}_{19}\text{H}_{30}\text{NO}_3$   $[\text{M} + \text{H}]^+$ , 320.2221,  $\Delta$  0.3 ppm).

**Cinnabaramide D (4):** white needles;  $[\alpha]_D^{20}$   $\pm 0$  ( $c$  0.5, MeOH); UV (MeOH)  $\lambda_{\text{max}}$  (log  $\epsilon$ ) 202 (4.05) nm; IR (ATR)  $\nu_{\text{max}}$  2929, 1722, 1656, 1374, 1240, 1197, 1143, 992, 825  $\text{cm}^{-1}$ ; NMR data, see Table 2; HRESIMS  $m/z$  370.2219 (calcd for  $\text{C}_{19}\text{H}_{32}\text{NO}_6$   $[\text{M} + \text{H}]^+$ , 370.2225,  $\Delta$  1.6 ppm).

**Cinnabaramide E (5):** white needles;  $[\alpha]_D^{20}$   $-23$  ( $c$  0.1, MeOH); UV (MeOH)  $\lambda_{\text{max}}$  (log  $\epsilon$ ) 201 (4.00) nm; IR (ATR)  $\nu_{\text{max}}$  2928, 1737, 1682, 1377, 1261, 1164, 1088, 1046, 992, 864  $\text{cm}^{-1}$ ; NMR data, see Table 2; HRESIMS  $m/z$  354.2281 (calcd for  $\text{C}_{19}\text{H}_{32}\text{NO}_5$   $[\text{M} + \text{H}]^+$ , 354.2276,  $\Delta$  1.4 ppm).

**Cinnabaramide F (6):** white, amorphous solid;  $[\alpha]_D^{20}$   $+37$  ( $c$  0.5, MeOH); UV (MeOH)  $\lambda_{\text{max}}$  (log  $\epsilon$ ) 202 (4.15), 234 (3.70) nm; IR (ATR)  $\nu_{\text{max}}$  2926, 1740, 1683, 1660, 1537, 1222, 1113, 1023, 1002, 822  $\text{cm}^{-1}$ ; NMR data, see Table 3; HRESIMS  $m/z$  499.2469 (calcd for  $\text{C}_{24}\text{H}_{39}\text{N}_2\text{O}_7\text{S}$   $[\text{M} + \text{H}]^+$ , 499.2473,  $\Delta$  0.8 ppm).

**Cinnabaramide G (7):** white, amorphous solid;  $[\alpha]_D^{20}$   $+24$  ( $c$  0.5, MeOH); UV (MeOH)  $\lambda_{\text{max}}$  (log  $\epsilon$ ) 202 (4.16), 230 (3.71) nm; IR (ATR)  $\nu_{\text{max}}$  2931, 1749, 1682, 1656 sh, 1530, 1362, 1221, 1170, 1112, 1045, 1005, 819  $\text{cm}^{-1}$ ; NMR data, see Table 3; HRESIMS  $m/z$  513.2617 (calcd for  $\text{C}_{25}\text{H}_{41}\text{N}_2\text{O}_7\text{S}$   $[\text{M} + \text{H}]^+$ , 513.2629,  $\Delta$  2.3 ppm).

**Acknowledgment.** We thank Dr. S. Wilhelm (Bayer West Haven), Dr. T. Satoh, S. Matsukawa, and K. Fuchikami (formerly of Bayer Yakuhi) for providing biological test data, and all other former colleagues of the Bayer Research Center Kyoto, for their support of the project. Prof. H. H. Fiebig (Oncotest, Freiburg, Germany) is thanked for confirmation of cytotoxic activities of cinnabaramides. The DSMZ culture collection (Braunschweig, Germany) is acknowledged for confirming the taxonomy of JS360 and for providing a reference strain. Our former colleague, Dr. Stephan Seip (Bayer HealthCare, Leverkusen, Germany), is acknowledged for his efforts regarding the structure elucidation of the cinnabaramides. Expert technical assistance by A. Rademacher, C. Wotsch, M. Benfer, S. Heke, and D. Müller (InterMed Discovery) is gratefully acknowledged.

**Supporting Information Available:** Table S1, providing HPLC  $t_R$  values, ESIMS data, and yields of cinnabaramides **1–7**; Tables S2–S8, summarizing the 1D and 2D NMR data of **1–7**; Figures S1–S7, showing  $^1\text{H}$  NMR spectra of **1–7**. In addition, a CIF file containing the X-ray data of compound **1** (corresponding to Figure 3) is provided. This material is available free of charge via the Internet at <http://pubs.acs.org>.

## References and Notes

- (1) Coux, O.; Tanaka, K.; Goldberg, A. N. *Ann. Rev. Biochem.* **1996**, *65*, 801–847.

- (2) Ciechanover, A. *Cell* **1994**, *79*, 13–21.
- (3) Kyle, R. A.; Rajkumar, S. V. *N. Engl. J. Med.* **2004**, *351*, 1860–1873.
- (4) Koguchi, Y.; Kohno, J.; Suzuki, S.; Nishio, M.; Takahashi, K.; Ohnuki, T.; Komatsubara, S. *J. Antibiot.* **1999**, *12*, 1069–1076.
- (5) (a) Koguchi, Y.; Kohno, J.; Nishio, M.; Takahashi, K.; Okuda, T.; Ohnuki, T.; Komatsubara, S. *J. Antibiot.* **1999**, *52*, 63–65. (b) Kohno, J.; Koguchi, Y.; Nishio, M.; Nakao, K.; Kuroda, M.; Shimizu, R.; Ohnuki, T.; Komatsubara, S. *J. Org. Chem.* **2000**, *65*, 990–995. (c) Tsukamoto, S.; Yokosawa, H. *Curr. Med. Chem.* **2006**, *13*, 745–754.
- (6) Tomoda, H.; Omura, S. *Yakugaku Zasshi* **2000**, *120*, 935–949.
- (7) (a) Feling, R.; Buchanan, G. O.; Mincer, T. J.; Kauffman, C. A.; Jensen, P. R.; Fenical, W. *Angew. Chem., Int. Ed.* **2003**, *42*, 355–357. (b) Williams, G. W.; Buchanan, G. O.; Feling, R. H.; Kauffman, C. A.; Jensen, P. R.; Fenical, W. *J. Org. Chem.* **2005**, *70*, 6196–6203.
- (8) Chauhan, D.; Catley, L.; Li, G.; Podar, K.; Mitsiades, C.; Mitsiades, N.; Yasui, H.; Letai, A.; Ovaa, H.; Berkers, C.; Nicholson, B.; Chao, T.; Neuteboom, S.; Richardson, P.; Palladino, M.; Anderson, K. C. *Cancer Cell* **2005**, *8*, 407–519.
- (9) Stadler, M.; Seip, S.; Müller, H.; Mayer-Bartschmid, A.; Brüning, M. A.; Benet-Buchholz, J.; Togame, H.; Dodo, R.; Reinemer, P.; Bacon, K.; Fujikami, K.; Matsukawa, S.; Urbahns, K. World Patent 2004,071,382, 2004.
- (10) Reference sequences were retrieved from GenBank (<http://www.ncbi.nlm.nih.gov>) by a similarity search using FASTA ([http://fasta.bioch.virginia.edu/fasta\\_www/cgi](http://fasta.bioch.virginia.edu/fasta_www/cgi)) program. The sequence obtained from JS360 was assigned the GenBank designation number AJ890475.
- (11) (a) Mincer, T. C.; Jensen, P. R.; Kauffman, C. A.; Fenical, W. *Appl. Environ. Microbiol.* **2002**, *60*, 5005–5011. (b) Maldonado, L. A.; Fenical, W.; Jensen, P. R.; Kauffman, C. A.; Mincer, T. J.; Ward, A. C.; Goodfellow, M. *Int. J. Syst. Evol. Microbiol.* **2005**, *55*, 1759–1766.
- (12) Crystallographic data for the structure reported in this paper have been deposited at the Cambridge Crystallographic Data Centre (deposition number CCDC-273651). Copies of the data can be obtained, free of charge, on application to the Director, CCDC, 12 Union Road, Cambridge CB2 1EZ, UK (fax: +44-(0) 1223-33603.3 or e-mail: [deposit@ccdc.cam.ac.uk](mailto:deposit@ccdc.cam.ac.uk)).
- (13) Fenteany, G.; Schreiber, S. L. *J. Biol. Chem.* **1998**, *273*, 8545–8548.
- (14) (a) Macherla, V. R.; Mitchell, S. S.; Manam, R. R.; Reed, K. A.; Chao, T. H.; Nicholson, B.; Deyanat-Yazdi, G.; Mai, B.; Jensen, P. R.; Fenical, W.; Neuteboom, S. T.; Lam, K. S.; Palladino, M. A.; Potts, B. C. *J. Med. Chem.* **2005**, *48*, 3684–3687. (b) Williams, P. G.; Buchanan, G. O.; Feling, R. H.; Kauffman, C. A.; Jensen, P. R.; Fenical, W. *J. Org. Chem.* **2005**, *70*, 6196–6203. (c) Hogan, P. C.; Corey, E. G. *J. Am. Chem. Soc.* **2005**, *127*, 15386–15387.
- (15) Groll, M.; Huber, R.; Potts, B. C. M. *J. Am. Chem. Soc.* **2006**, *128*, 5136–5141.
- (16) (a) Corey, E. J.; Li, W.; Nagamitsu, T. *Angew. Chem., Int. Ed.* **1998**, *37*, 1676–1678. (b) Reddy, L. R.; Saravanan, P.; Corey, E. J. *J. Am. Chem. Soc.* **2004**, *126*, 6230–6231. (c) Endo, A.; Danishefsky, S. J. *J. Am. Chem. Soc.* **2005**, *127*, 8298–8289. (d) Reddy, L. R.; Fournier, J. F.; Reddy, B. V.; Corey, E. J. *Org. Lett.* **2005**, *7*, 2699–2701.
- (17) Hillebrand, S.; Guth, O.; Wiese, W.-B.; Kunz, K.; Kullmann, A.; Mattes, A.; Schreier, P.; Wachendorff-Neumann, U.; Kuck, K.-H.; Lösel, P.; Malsam, O.; Reinemer, P.; Stadler, M.; Seip, S.; Mayer-Bartschmid, A.; Müller, H.; Bacon, K. World Patent 2006,005,551, 2006.
- (18) Sheldrick, G. M. *SHELXL97*, Program for the Refinement of Crystal Structures; University of Göttingen: Germany, 2001.
- (19) Marfey, P. *Carlsberg Res. Commun.* **1984**, *49*, 591–596.

NP060162U